Stability Analysis of the Second Order Σ–Δ Modulator

Philip Steiner and Woodward Yang

Division of Applied Sciences, Harvard University
Cambridge, MA

Abstract

The stability of the second order Σ–Δ modulator proposed by Candy [1] is proven for any properly bounded DC input. It is found, however, that there exists a class of AC inputs for which this Σ–Δ modulator is unstable over most of the dynamic range of the input. The possible extension of the methods used for the second order system to higher order systems is discussed as well.

Introduction

Σ–Δ systems are basically clocked linear systems with the addition of a single nonlinearity introduced by the quantizer which can be modeled as a thresholding function in the dynamical equations. Due to this nonlinearity, direct application of linear systems analysis has not been able to yield closed form solutions of these nonlinear dynamical equations. One analysis technique is to model the quantizer as a linear gain element with additive quantization error. This error is viewed as a noise source, and the system can then be analyzed using standard linear system techniques. Analyses of this type, though useful, have not been able to model the system behavior well enough to predict the stability and performance of a given design, and simulation has remained the main tool in the design and testing of Σ–Δ modulators.

In attempting to better predict the behavior of Σ–Δ modulators, various nonlinear analysis techniques have been applied and have yielded promising results [3,4,5]. In this paper, we utilize an analysis method which circumvents the difficulty introduced by the thresholding function by segmenting the state space into regions in which the modulator output is constant. This eliminates the nonlinearity and reduces the dynamical equations to simple linear systems within each of the segmented regions. Thus, the linear behavior of the system in each region along with a description of the transition mechanism between regions completely characterizes the dynamics of the second order modulator. Using this technique, we are able (i) to prove that the second order modulator is stable for all properly bounded DC inputs and (ii) to provide relatively simple, analytical, expressions for the maximum and minimum values of the integrator outputs. In particular, we define the stability of the Σ–Δ modulator in terms of a compact region that contains all possible integrator values after sufficiently long times.

Problem Definition

The system of interest in this paper is the second order Σ–Δ modulator proposed by Candy [1] which is shown in Figure 1 (note that in the following three sections we consider the system for which $\alpha = \beta = 1$).

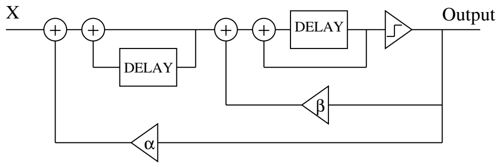

Figure 1: A general second order Σ–Δ modulator.

The two independent states of the system are taken to be the outputs of the two integrators and are labeled S_1 and S_2. The dynamical equations governing the evolution of the system are then given by

$$\begin{aligned} S_1(n+1) &= S_1(n) + X(n+1) - \Theta(S_2(n+1)) \quad (1)\\ S_2(n+1) &= S_2(n) + S_1(n) - \Theta(S_2(n)) \end{aligned}$$

$$\text{where: } \Theta(y) = \left\{ \begin{array}{ll} +1 & \text{if } y \geq 0 \\ -1 & \text{if } y < 0 \end{array} \right\}$$

and the input, $X(n+1)$, is bounded by the range of the thresholding function so that $-1 < X(n+1) < 1$.
The state space of this system is a plane with S_1 as the horizontal axis and S_2 as the vertical axis as shown in Figure 2. This plane can be segmented into four distinct regions (labeled I through IV), two in the upper half-plane and two in the lower half-plane. In each of these regions the thresholding functions in equation (1) take on only a single value and equations (1) reduce to a linear system in each region. In region I for example, $\Theta(S_2(n+1)) = +1$ and $\Theta(S_2(n)) = +1$. The nonlinearity only becomes evident as the system makes transitions between regions.

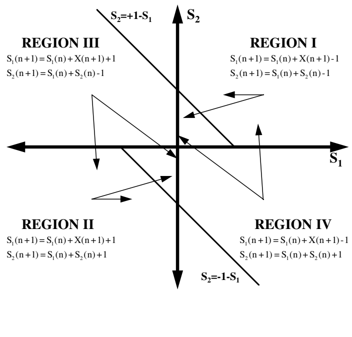

Figure 2: The state space segmented into four regions (I - IV) with linear dynamical behavior.

[1]This work was supported in part by an NSF Young Investigator Award (MIP-92-57964), an Army Research Office Young Investigator Award (DAAL03-92-G-0375), and a grant from the George W. Merck Foundation at Community Funds. In addition, P. Steiner was supported in part by a fellowship from the Quebec government FCAR program.

Transitions between the upper and lower half-planes occur when the system occupies a point in either of regions III or IV. Figure 2 shows the mapping of the states (here we consider a state as the coordinate (S_1, S_2)) in each region. For example states in region I map to states in either region I or region III and never to states in region II or region IV. Also shown in Figure 2 are the linear equations which apply to states in each region. States in the upper half-plane which directly evolved from a state in the lower half-plane as well as states in the lower half-plane which directly evolved from a state in the upper half-plane are called *transition points* because the system has jumped from one half-plane to the other. Note from Figure 2 that transition points can occur in any of the four regions.

Dynamics of the System

In this section we consider DC inputs to the modulator so that the $X(n+1)$ in equation (1) reduces to a constant DC value, X. Figure 3 shows a simulation of the time evolution of the states of a second order Σ–Δ modulator.
This evolution consists of cycles of a set of states in the upper half-plane followed by a transition to the lower half-plane, a set of states in the lower half-plane, and finally a transition back to the upper half-plane where the cycle begins again. Consider for the moment only the set of states in a single cycle which lie in the upper half-plane (shown in Figure 3). All these points fall on a parabola given by the equation

$$S_2 = \frac{1}{2(X-1)}(S_1^2 - (1+X)S_1 + D_1) \tag{2}$$

where the constant D_1 parameterizes all possible trajectories in the upper half-plane. Once the system makes a transition to the lower half-plane, all the states in that part of the cycle fall on a parabola given by

$$S_2 = \frac{1}{2(X+1)}(S_1^2 - (X-1)S_1 + D_2) \tag{3}$$

where the constant D_2 again parameterizes all possible trajectories in the lower half-plane. Note that the family of parabolas in each of the half-planes are nonintersecting and define the locus of all possible state values between two transition points.

The dynamics of the system can therefore be characterized by specifying the list $D_1^1, D_2^1, D_1^2, D_2^2, \ldots$ of constants. In practice, complexity of the constants increases rather quickly, and it is difficult to specify this list analytically due to the algebraic complexity.

Stability of the System

We prove the stability of the second order modulator using a two step approach which is outlined below.

(i) We show that there exists a region A, such that once the system occupies a state inside A, it will remain inside of A at all future time steps. The region A is called the *compact region.* i.e.

$$\exists\, A \mid (S_1(n), S_2(n)) \in A \Rightarrow (S_1(n+k), S_2(n+k)) \in A \;\forall k = 1, 2, \ldots$$

(ii) We show that for arbitrary initial conditions, there exists a $(S_1(n), S_2(n))$, with n finite, such that $(S_1(n), S_2(n)) \in A$. In other words, the system will reach the compact region from arbitrary initial conditions in a finite number of time steps.

The motivation behind using this method lies in the fact that it can be easily applied to the second order system as well as its possible applicability to higher order systems.

Defining the Compact Region

A description of how the compact region is found is beyond the scope of this paper, and we merely mention that the compact region, A, for the second order modulator (with $\alpha = \beta = 1$) does exist and is given by

$$A = [(S_1, S_2) \in \Re^2 \mid -2 + X < S_1 < 2 + X;\; g(S_1) < S_2 < f(S_1)] \tag{4}$$

with the functions $g(S_1)$ and $f(S_1)$ given by

$$f(S_1) = \frac{1}{2(X-1)}(S_1^2 - (X+1)S_1 + 3X - 6) \tag{5}$$
$$g(S_1) = \frac{1}{2(X+1)}(S_1^2 - (X-1)S_1 - 3X - 6)$$

The shape of the compact region depends upon the value of the DC input, X. Figure 4 shows the compact region for $X = 0.0$. Note that the compact region is made up of two parabolas of the form of equations (2) and (3) with the values

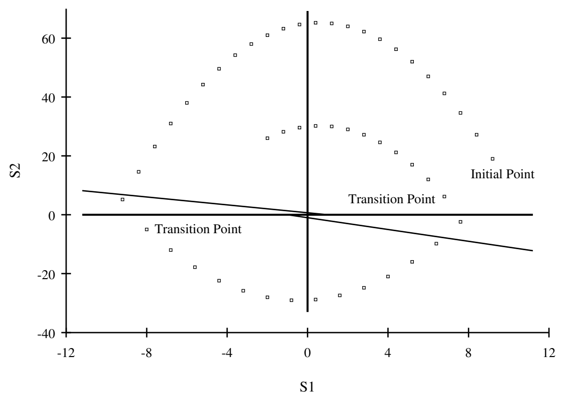

Figure 3: System dynamics of the second order modulator.

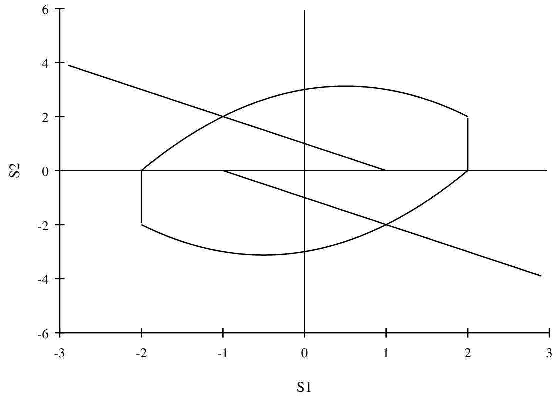

Figure 4: Compact region for DC input, $X = 0$.

of the constants set to $D_1 = 3X - 6$, $D_2 = -3X - 6$. With the compact region thus defined it can be shown that A satisfies requirement (i) in the list above, that is

$$(S_1(n), S_2(n)) \in A \Rightarrow (S_1(n+k), S_2(n+k)) \in A \; \forall k = 1, 2, \ldots$$

Once the system is inside the compact region, it is clear from equation (4) that the states (outputs of the integrators) are bounded.

Reaching the Compact Region

Proving that the system will reach the compact region in a finite number of time steps from arbitrary initial conditions relies on certain properties of the parabolas in equations (2) and (3). The essential details are expressed in Figure 5. Starting from initial conditions (A_0, B_0), outside of the compact region and in the upper half-plane, the resulting sequence of states in the upper half-plane will lie on a parabola of the form given by equation (2) and parameterized by D_1. Equivalently, the parabola can also be parameterized by its left intercept with the x-axis, (N_0,0), as shown in Figure 5a. When the system reaches region III, it will make a transition to the lower half-plane where subsequent states will lie on a parabola of the form of equation (3). However, as shown in Figure 5a and 5b, there is a range of possible transition states and trajectories which will depend on the exact value of the initial conditions. When the system reaches region IV, it will make a transition back to the upper half-plane, and the resulting locus of possible transition states is shown in Figure 5c. The subsequent sequence of states in the upper half-plane will lie on a new parabola which can be parameterized by its left intercept, (N_1,0), as shown in Figure 5d. It is possible to show that even the worst case transitions will result in a lower bound on the difference $N_n - N_{n+1}$ that is sufficiently large to guarentee that the system state will reach the compact region in a finite number of time steps.

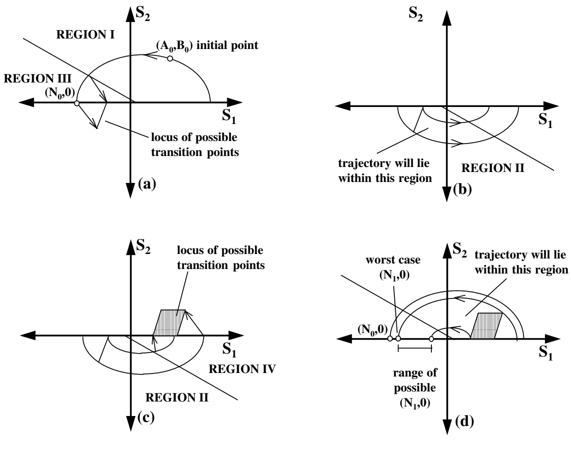

Figure 5: System dynamics with DC input and arbitrary initial conditions (A_0, B_0), outside of the compact region.

By demonstrating both steps of the proof as outlined above it is seen that the second order Σ–Δ modulator is stable for all DC inputs bounded by the range of the quantizer function.

General Feedback Parameters

The above discussion concentrated on the system for which $\alpha = \beta = 1$ in Figure 1. The analysis for systems in which the feedback parameters take on values other than unity is similar to the one just presented with the proviso that not all of these systems are stable. The analog of equation (4) for the general system is

$$A = [(S_1, S_2) \in \Re^2 \mid M_1 < S_1 < M_2;\; g\prime(S_1) < S_2 < f\prime(S_1)] \quad (6)$$

Figure 6 shows the compact region for $\alpha/\beta = 4/3$ with $X = 0$.

The analysis of this system follows on exactly the same lines as the one presented above except for being much more involved algebraically. In addition, the stability of a system with a particular choice for α and β may depend on the value of the DC input. For some choices of the feedback parameters the system is stable only for some limited range of the input (smaller than the range of the quantizer function).

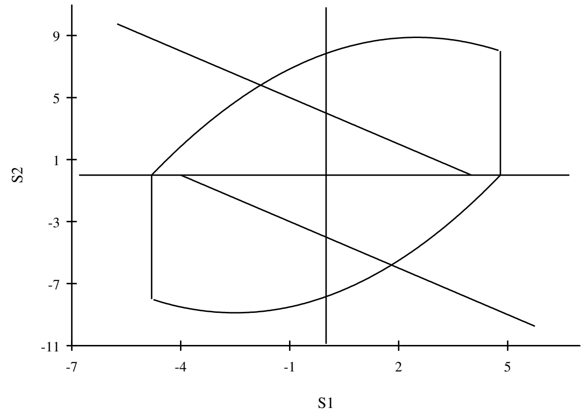

Figure 6: Compact region for the general system $\alpha/\beta = 4/3$ and X=0.0

Instability for AC Input

In this section, we again consider the system for which $\alpha = \beta = 1$. It was seen that this modulator is stable for all DC inputs in the range $-1 < X < 1$. Consider the AC input, bounded in the range $-P < X(n+1) < P \; \forall n$ with $0 < P < 1$, defined below

$$X(n+1) = \left\{ \begin{array}{ll} +P & \text{if } S_2(n) \geq 0 \text{ and } S_1(n) > 1 \text{ or} \\ & S_2(n) < 0 \text{ and } S_1(n) \geq -1 \\ & \\ -P & \text{if } S_2(n) \geq 0 \text{ and } S_1(n) \leq 1 \text{ or} \\ & S_2(n) < 0 \text{ and } S_1(n) < -1 \end{array} \right\} \quad (7)$$

It is seen in simulation that this input drives the modulator to arbitrarily large state values for values of P as small as 0.2 as shown in Figure 7. Thus, there exists a class of AC inputs for which the modulator is unstable. While equation (7) does represent a contrived input which might not arise in real signals, the instability of the modulator over such a large portion of the input dynamic range seems to suggest that there might be more general class of AC inputs for which the modulator is unstable. This clearly demonstrates that the second order modulator is not unconditionally stable for arbitrary AC inputs. The stability of the modulator for band-limited signals is currently under investigation.

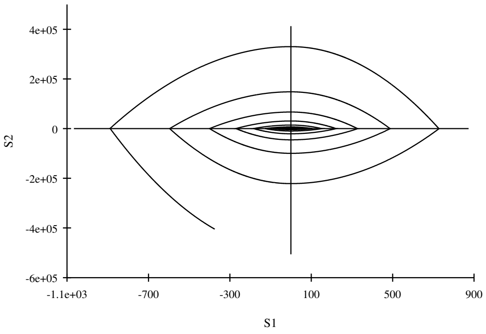

Figure 7: Simulation of system instability for "worst case" AC input with P=0.2.

Higher Order Systems

It should be possible to extend the analysis presented in the previous section directly to higher order interpolative modulators. The main difficulty in doing this is that the algebraic complexity of the analysis increases in direct proportion to the order of the modulator.

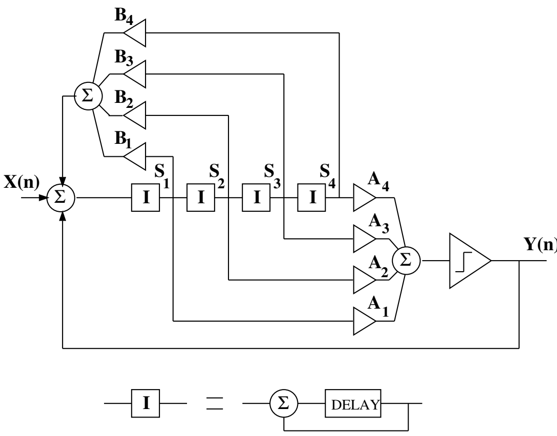

Figure 8: A fourth order modulator.

The fourth order modulator shown in Figure 8 is a slightly modified version of the one presented in reference [2] and has been shown to be stable in simulations. The most important features of this system are the linear feedback paths. Previous linear analysis of these feedback paths suggest that they are responsible for system stabilization. In addition, the nonlinear analysis of higher order systems with these paths can be simplified as follows.

The dynamic equations of the modulator are given in matrix form as

$$\begin{pmatrix} S_1 \\ S_2 \\ S_3 \\ S_4 \end{pmatrix}_{n+1} = \begin{bmatrix} 1-B_1 & B_2 & B_3 & B_4 \\ 1 & 1 & 0 & 0 \\ 0 & 1 & 1 & 0 \\ 0 & 0 & 1 & 1 \end{bmatrix} \begin{pmatrix} S_1 \\ S_2 \\ S_3 \\ S_4 \end{pmatrix}_n + \begin{pmatrix} 1 \\ 0 \\ 0 \\ 0 \end{pmatrix} X(n) + \begin{pmatrix} 1 \\ 0 \\ 0 \\ 0 \end{pmatrix} \Theta[\sum_k A_k S_k(n)] \tag{8}$$

We can transform co-ordinates (for $B_i > 0, i \geq 2$) to *canonical* co-ordinates in which the dynamical equation takes the form

$$\begin{pmatrix} S_1 \\ S_2 \\ S_3 \\ S_4 \end{pmatrix}'_{n+1} = \begin{bmatrix} a_1 & 0 & 0 & 0 \\ 0 & a_2 & 0 & 0 \\ 0 & 0 & a_3 & 0 \\ 0 & 0 & 0 & a_4 \end{bmatrix} \begin{pmatrix} S_1 \\ S_2 \\ S_3 \\ S_4 \end{pmatrix}'_n + \begin{pmatrix} b_1 \\ b_2 \\ b_3 \\ b_4 \end{pmatrix} X(n) + \begin{pmatrix} c_1 \\ c_2 \\ c_3 \\ c_4 \end{pmatrix} \Theta[\sum_k d_k S'_k(n)] \tag{9}$$

where the a_i, b_i, c_i may be complex variables.

In this co-ordinate system, the state variables are related to each other only through the quantizer function. This simplifies the analysis when the system's state space is divided into separate linear systems. Furthermore, it is clear that a large number of Σ–Δ modulator architectures with a variety of feedforward and feedback paths between integrators can be transformed into this canonical form. In particular, the only requirement is that the linear system formed by the integrators must be similar to a diagonal matrix as shown above.

Conclusions

The second order Σ–Δ modulator shown in Figure 1 can be well understood by utilizing the nonlinear analysis described above. The essential technique of this analysis is to segment the state space of the system into regions where the dynamical equations are linear, and then to describe the mapping from region to region. A closed form proof of the stability of the second order modulator follows directly. Furthermore, by transforming higher order systems into a canonical form, this nonlinear analysis can also be applied to higher order systems.

Currently, this analysis is being extended to study the effects due to nonideal components and how they influence system stability and coding/decoding performance.

References

[1] J.C. Candy. "A Use of Double Integration in Sigma Delta Modulation.", *IEEE Trans. Commun.* , March 1985

[2] K.C.H. Chao, S. Nadeem, W.L. Lee, C.G. Sodini, "A Higher Order Topology for Interpolative Modulators for Oversampling A/D Converters.", *IEEE Trans. on Circuits and Systems*, March 1990

[3] Soren Hein and Avideh Zakor, "On the Stability of Sigma Delta Modulators", *IEEE DSP Workshop*, New York, Sept. 1990

[4] Hongmo Wang, "A Geometric View of Sigma Delta Modulation", *IEEE Trans. on Circuits and Systems*, June 1992

[5] Steven Pinault, *Private Communication*